Society For Biomaterials

In vivo evaluation of an elastomeric small-diameter vascular graft reinforced with a highly flexible Nitinol mesh

Giorgio Soldani,[1] Michele Murzi,[2] Francesco Faita,[3] Nicole Di Lascio,[3,4] Tamer Al Kayal,[1] Raffaele Spanò,[5†] Barbara Canciani,[5‡] Paola Losi[1]

[1]Laboratory for Biomaterials & Graft Technology, Istituto di Fisiologia Clinica CNR, Massa 54100, Italy
[2]Fondazione Toscana Gabriele Monasterio (FTGM), Massa 54100, Italy
[3]Laboratory for Experimental Ultrasound, Istituto di Fisiologia Clinica CNR, Pisa 56127, Italy
[4]Institute of Life Sciences, Scuola Superiore Sant'Anna, Pisa 56127, Italy
[5]Laboratory of Regenerative Medicine, DIMES, University of Genoa, Genoa 16132, Italy

Received 26 October 2017; revised 22 May 2018; accepted 12 June 2018
Published online 3 September 2018 in Wiley Online Library (wileyonlinelibrary.com). DOI: 10.1002/jbm.b.34189

Abstract: Highly porous small-diameter vascular grafts (SDVGs) prepared with elastomeric materials such as poly(ether urethane) (PEtU)–polydimethylsiloxane (PEtU-PDMS) are capable to biodegrade but may develop aneurismal dilatation. Through a compliance/patency assessment with ultrasound techniques, the current study investigated the functionality, in terms of patency and endothelialization, of a highly flexible and porous Nitinol mesh incorporated into PEtU-PDMS SDVGs in a sheep carotid model. Nitinol-PEtU-PDMS grafts with an internal diameter (ID) of 4 mm were manufactured by spray, phase-inversion technique. Compliance tests were performed by ultrasound (US) imaging using a high-resolution ultrasound diagnostic system. Ten adult sheep were implanted with 7 cm long grafts. The results of this study demonstrated an almost complete neointima luminal coverage in transmurally porous grafts reinforced with the Nitinol meshes after 6 months of implantation. Additionally, ultrasound has been used to quantitatively assess and monitor hemodynamic variables in an experimental model of synthetic vascular graft replacement. The use of reinforced PEtU-PDMS grafts may accelerate the endothelialization process of relatively long grafts, such as those needed for aortocoronary bypass. © 2018 Wiley Periodicals, Inc. J Biomed Mater Res Part B: Appl Biomater 107B: 951–964, 2019.

Key Words: small-diameter vascular graft, poly(ether-urethane)–polydimethylsiloxane, flexible nitinol mesh, in vivo evaluation, endothelialization

How to cite this article: Soldani G, Murzi M, Faita F, Di Lascio N, Al Kayal T, Spanò R, Canciani B, Losi P. 2019. In vivo evaluation of an elastomeric small-diameter vascular graft reinforced with a highly flexible Nitinol mesh. J Biomed Mater Res Part B 2019:107B:951–964.

INTRODUCTION

Coronary artery disease is characterized by a progressive reduction of the caliber (stenosis) of one or more epicardial coronary arteries leading to a reduction of the coronary flow reserve. This consequently results in an imbalance between supply and request of oxygen even when resting.[1] Approximately 550,000 people die from coronary heart disease each year and 5.4 million new cases are diagnosed. Coronary heart disease is in fact the leading cause of death in developed countries.[2] The treatment of coronary artery disease has evolved considerably in recent years and now includes drug therapy, percutaneous treatment of coronary lesions and, in the most severe cases, surgical therapy with a coronary artery bypass graft (CABG).[3] Currently the majority of coronary artery bypass interventions are carried out using the left internal mammary artery or segments of the autologous saphenous vein.[4] However, a significant number of patients do not have venous conduits of adequate quality, due to the presence of associated venous disease or a previous saphenectomy. Therefore, it would be extremely important to have an off-the-shelf, synthetic, small-diameter vascular graft (SDVG) for coronary artery bypass interventions.

One important aspect for the success of SDVGs is the possibility to achieve rapid endothelialization to prevent thrombus formation. In the endothelialization process, porosity plays a key role in the structure of the graft, in terms of pore size and size distribution. Since the 1960s, numerous studies have highlighted the importance of graft porosity. Now it is generally accepted that a porous inner surface is necessary to anchor the neointima in position, while a porous outer surface is essential to promote the

[†]Present address: Department of Drug Discovery and Development, Istituto Italiano di Tecnologia, Via Morego, 30, Genova 16163, Italy
[‡]Present address: Department of Biomedical Sciences for Health, Università degli studi di Milano, via Mangiagalli 31, 20133, Milano, Italy
Correspondence: G. Soldani; e-mail: giorgio.soldani@ifc.cnr.it
Contract grant sponsor: Kips Bay Medical, Inc.

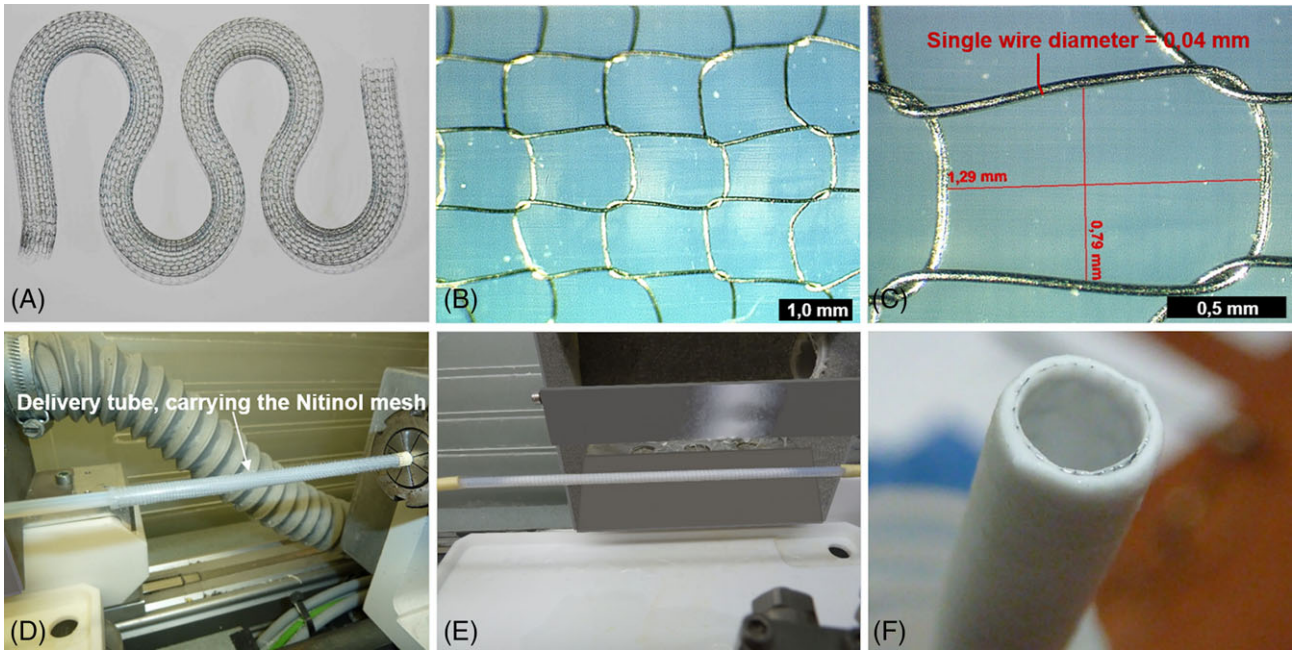

FIGURE 1. View of the eSVS Nitinol mesh and fabrication of the reinforced small-diameter vascular graft (SDVG). A: Macrophotography of the Nitinol mesh showing its pliability features. B: Stereomicroscope image of a mesh portion showing its characteristic Nitinol wire woven structure. C: Detail of the opening of the mesh between adjacent Nitinol wires, measuring approximately 1.29 mm in the longitudinal direction and 0.79 mm in the radial direction. The diameter of the wire is 40 μm (O.M. 60×). D: Positioning of the fluorinated ethylene propylene delivery tube, carrying the Nitinol mesh, on the mandrel to be successively spray-coated with the PEtU-PDMS material (white arrow). E: Spray-coating of the Nitinol mesh slided on a deposited initial layer of PEtU-PDMS material. F: Cross-section of the final reinforced graft with the incorporated Nitinol mesh.

infiltration of perigraft tissue, which will hold the prosthesis in place, prevent kinking, and provide a tissue substrate for the fibrinous luminal layers.[5] Unfortunately, grafts with a porous and compliant structure, such as that obtainable with polyurethane materials, can become mechanically weak over time and due to the radial internal pressure, may undergo aneurysmal dilatations. Therefore, one possible solution to solve this problem is to apply external reinforcement to the vascular graft.

Since the late 1990s, several attempts have been made to apply reinforcement technologies to vascular grafts made of polyurethane material. One of the first attempts to reinforce a 6.0 mm ID microporous polyurethane vascular graft was by an external polyester tubular knitted mesh which was reported by Eberhart et al. in 1999.[6] In this study, grafts were made of three polyurethanes of different chemistry, microphase separation, and mechanical properties. Another experiment performed by Xu et al. in 2010[7] referred to a composite polyurethane vascular graft with a small inner diameter of 4.0 mm. This was fabricated by reinforcing the microporous structure of the thin wall with a weft-knitted tubular fabric. A subsequent study by Yang et al. in 2012[8] reported the use of polyurethane vascular grafts, with internal diameters of 3.0, 4.0, and 5.0 mm, with coaxial three-layer wall thickness and reinforced with polyester/spandex fabric of different blend ratios. The studies mentioned above all evaluated the radial tensile property and compliance of SDVG in vitro, with or without the reinforcement with polyester tubular fabrics, but none of them described the performance of polyurethane reinforced grafts in vivo.

In 2010, Xie et al.[9] published the first study about in vivo evaluation of polyurethane reinforced grafts. In the study of Xie et al. three types of polyurethane grafts, featuring five different structural designs and chemical compositions, were compared in terms of device function, healing characteristics, and material stability in a canine abdominal aorta model (6.0 mm ID) for a period of 1 and 6 months. Graft morphological structures were either fibrillar or microporous with or without mechanical reinforcement. This ranged from an external polyester mesh to an integrated polyester monofilament, or to a built-in impervious polyurethane layer. Although Xie et al. reported that the overall performance of the studied grafts was rather unsatisfactory; they showed marked differences in the behavior of grafts with different structural designs. Grafts with a multilayer filamentous interconnected porous structure and reinforced on the outside by a polyester mesh showed the best results in terms of relatively thin, uniform, and partially endothelialized inner surfaces with good tissue in-growth, as compared to grafts with low-porosity or impervious walls, both with or without reinforcement.

Recently, a mesh made of Nitinol wire [Figure 1(A–C)], called eSVS Mesh (external Saphenous Vein Support, Kips Bay Medical, Inc., Minneapolis, MN[10]) designed to prevent overexpansion of saphenous venous grafts under arterial pressure, was tested in our center as part of a multicenter randomized clinical trial. The eSVS Mesh study aimed to

evaluate the safety and the effectiveness of the eSVS Mesh for coronary artery bypass.[11]

Owing to established experiences in SDVGs fabrication and evaluation[12] and the recent clinical experience gained from the eSVS Mesh study,[11] in this work, we wanted to investigate the feasibility of incorporating the eSVS Nitinol mesh into the wall of a synthetic SDVG. The rationale for this study was that this reinforced graft would be able to avoid aneurysmal graft dilatation[12] and, at the same time, allow increased porosity of the graft wall for better tissue integration, without the risk of reducing graft structural strength.

Indeed, another important aspect when dealing with SDVGs is their mechanical incompatibility with native vessels leading to wall weakening, anastomosis dilatation, thrombus formation, and intimal hyperplasia.[13] However, this incompatibility can be strongly avoided reducing the compliance mismatch between SDVGs and natural arteries.[14]

Thus, the aim of this study was to evaluate functionality, in terms of degree of patency and endothelialization, of highly porous poly(ether)urethane (PEtU)-polydimethylsiloxane (PDMS) SDVGs incorporating the eSVS Nitinol mesh implanted in the common carotid artery sheep model using the CABG technique.

EXPERIMENTAL STUDY

Graft material preparation

The chemical reaction between a medical grade, aromatic, PEtU (Estane 5714, Lubrizol Advanced Materials, Inc., Cleveland, OH) and a diacetoxy silyl terminated (tetraacetoxy functional) PDMS (United Chemical Technologies, Inc., Bristol, PA) was carried out as previously described.[15,16] In particular, a 30% PDMS solution with respect to PEtU was added to the reaction mixture.

The 3% (w/v) PEtU-PDMS final solution in 1:1 (v/v) tetrahydrofurane (THF):1,4-dioxane (DX) was stored at room temperature protected from light until use.

PEtU-PDMS graft manufacturing

PEtU-PDMS vascular grafts were manufactured according to a previously described spray, phase-inversion technique.[17,18] Briefly, this technique allows to fabricate tubular microporous structures by simultaneously spraying a polymeric solution and a nonsolvent (aqueous solution) onto a Teflon rotating mandrel. The interaction between solvent and nonsolvent induces a sudden phase-inversion effect on the polymer that, consequently, precipitates from the solution. This phenomenon makes possible the subsequent deposition of porous microfibrillary layers of material over a rotating spindle.

In this study, a 3% (w/v) PEtU-PDMS stock solution was diluted with 1:1 THF/DX in order to obtain a 0.2% working solutions. Then the 0.2% solution was brought close to the point of precipitation by the addition of 17% (v/v) of distilled H_2O.

Grafts, 8.0 cm in length, 4.0 mm I.D., and approximately 350 μm in wall thickness were manufactured featuring a highly porous structure along the graft wall, which was obtained by co-spraying with a 0.2% (w/v) PEtU-PDMS solution and distilled water. During the fabrication process, a highly flexible Nitinol mesh (eSVS Mesh, kindly supply by Kips Bay Medical, Inc., Minneapolis, MN) was incorporated into the graft wall by a fluorinated ethylene propylene delivery tube [Figure 1(D–F)]. Thereafter, the graft was immersed in distilled H_2O overnight to allow solvent removal.

Finally, grafts were removed from the mandrel by an axial stretching of the Teflon mandrel and stored in wet conditions at 4°C until implantation.

Morphological analysis

Graft microgeometry was examined by Sudan Black staining with a procedure previously described.[19] Briefly, graft samples were dipped in a staining solution (0.12% w/v in absolute ethanol) for 10 min and then rinsed in distilled water. The stained surfaces were observed using a stereomicroscope (SZH0, Olympus, Milan, Italy), representative images were acquired by a video camera (KY-F32, JVC, Milan, Italy) at 40× magnification and analyzed by a computerized image analysis system (KS 300–3.0, Zeiss, Jena, Germany). In particular, circles were manually drawn following the perimeter of visible porous, then the software calculated the average diameter ± standard deviation.

The hydraulic permeability was characterized by measurement of the volume of degassed distilled water collected in the first minute by filtration through the graft wall at the standard transmural pressure of 120 mmHg.

In vitro compliance evaluation

All in vitro compliance tests were performed by ultrasound (US) imaging using a high-resolution US diagnostic system (Mylab 25, Esaote, Italy) equipped with a linear 7.5 MHz transducer. The values of the area and of the pressure were obtained following inserting the Nitinol mesh reinforced graft into the experimental circuit schematized in Figure 2 (A), which allowed the measurement of the diameter of the graft by means of ultrasound image analysis when different ranges of pressure were applied. Graft compliance was evaluated by analyzing the slope of the area–pressure curve. Unfortunately, it was not possible to obtain meaningful data about the compliance of unreinforced grafts since the weak and thin wall of the graft experienced overexpansion with minimal pressure changes.

In short, the circuit was constituted by a VAD (VAD System, Medos GmbH) that worked as a pump allowing the water to flow in the circuit and through the graft at different pressure and frequency values emulating the real blood pressure wave. The pressure was varied between 50 and 160 mmHg, while the frequency was set to 40 bpm. The flow chamber of a previously developed bioreactor was used both to connect the graft to the hydraulic circuit and to keep the graft immersed in water [Figure 2(B)]. A water bath was needed to adapt the acoustic impedance between the graft and the ultrasound probe. The circuit included resistance elements and compliances in order to better emulate the behavior of the arterial circulatory system. A syringe was used for filling the circuit with water. The diameter of the vessel was obtained from analysis of ultrasound images as

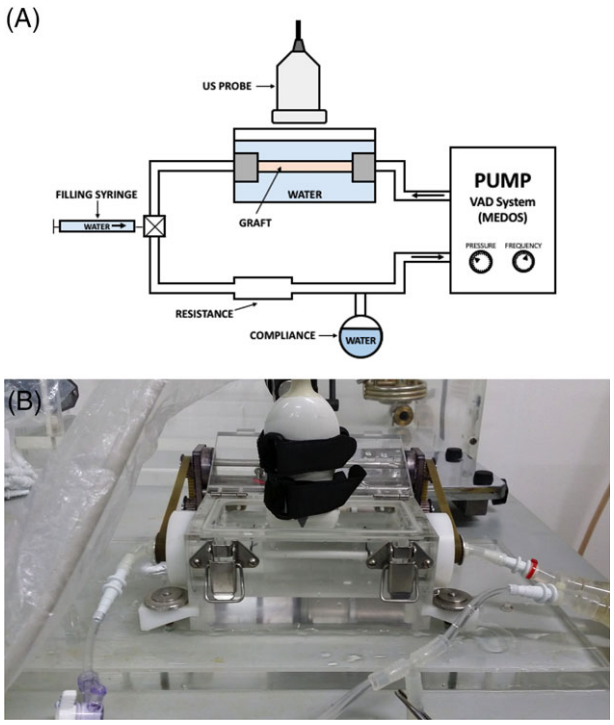

FIGURE 2. A: Schematic diagram of the in vitro compliance pulsatile test setup. Water can be inserted in the circuit through a filling syringe. A VAD system pump water in the circuit, which is composed by connecting tubes, resistance, compliance, and testing graft. The graft is contained in a flow chamber and immersed in water. B: Details of the flow chamber with the graft coupled with the ultrasound probe by water bath. The probe was held in a fixed position by using a mechanical probe holder. The graft is fully immersed in water in order to adapt the acoustic impedance and allowing the use of the ultrasound probe.

previously described.[20] Briefly, the maximum value of the diameter was obtained using automatic contour tracking techniques. We hypothesized that the maximum diameter was reached when the pressure was maximal, as indicated by the VAD gauge. Diameter and pressure values were plotted and all points were interpolated linearly. The slope of the fitted line was considered as the approximation of the compliance of the graft. This is possible because the compliance has an inverse relationship with the elastic Young modulus which can be obtained from the first derivative of the diameter versus pressure loop.[21]

Graft implantation

Ten adult sheep with a body weight of about 60 kg were used for this study. All animals received humane care according to guidelines from the Department of Food, Nutrition and Veterinary Public Health—Ministry of Health which approved this study (decree N. 48/2014-B), based on the Italian Legislative Decree 116/92 regarding animal experimentation.

Anesthesia was induced by spontaneous breathing with 48% O_2, 50% N_2O, and 2% isoflurane. Then the anesthesia was deepened with Propofol (Diprivan) 1 mg/kg and maintained with 30% O_2, 70% N_2O, isoflurane, and intravenous infusion of Propofol (2 mg/kg/h). Arterial blood pressure, blood gas and electrolytes were monitored by a catheter in the central ear artery and electrocardiographic monitoring by four electrode plates positioned at the limb extremities.

A 10-cm long longitudinal median incision in the neck was made by a scalpel blade to expose the left carotid artery. After heparinization (3 mg/kg) blood flow was measured. Grafts were cut with molded double flute beak ends with the distance of 7 cm between the molded ends. Immediately after, grafts were immersed in anticoagulated blood (heparin, Clexane, 5 U/mL) for 10 min.

The implant technique used was a double end-to-side anastomosis with carotid resection. Sutures were performed by everting technique with Prolene 7/0 [Figure 3(A)]. The graft naturally lay down, without traction, because of intrinsic arterial elasticity [Figure 3(B)]. At the end of the intervention, heparin was not neutralized, the muscular bend was sutured with Vicryl and the skin was sutured with Dexon 2/0 whipping.

Aspirin (325 mg) was administered daily for 3 days before intervention, and 100 mg/day till the end of the experimental period. Enrofloxacina (Baytril) and Fynadine 2 mL/45 kg were given as antibiotic and analgesic therapy, respectively. The animals' general health was checked daily.

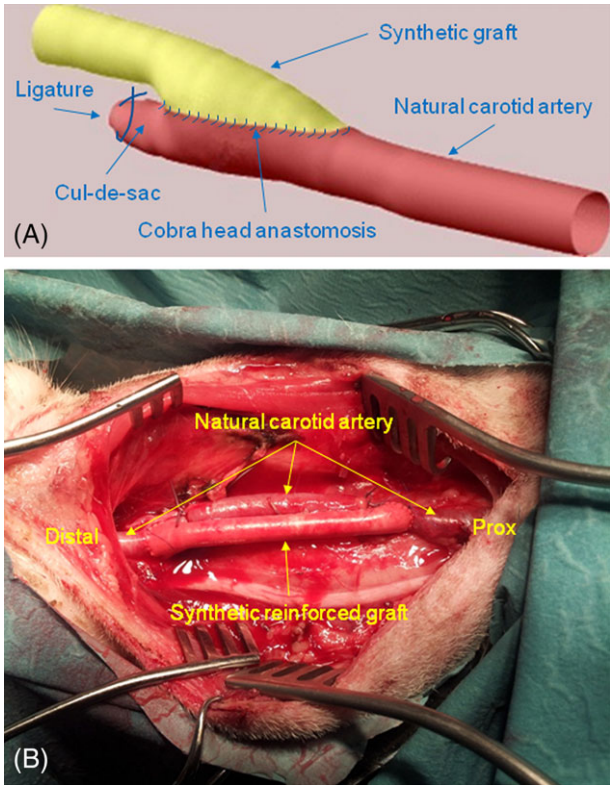

FIGURE 3. (A) Schematic representation of the "cobra head anastomosis" used in the implant technique of the graft; (B) view of the operating area after the Nitinol mesh reinforced graft implantation, according to the end-to-side anastomosis technique with carotid resection. The figure shows the carotid artery not yet resected and positioned below the graft.

Follow-up of graft patency and compliance by ultrasound imaging

All animals were monitored by the same high-resolution US diagnostic system employed for in vitro tests.[20] B-mode, Pulsed-Wave Doppler (PW-Doppler) and Color Doppler images were acquired in order to determine patency of the implanted grafts as well as to assess compliance and morphological characteristics of both operated and unoperated contralateral carotids.

Animals were positioned on the left/right side during ultrasound acquisitions. The head was held in a fixed position by manual constraint with the jaw and the neck forming a 150° angle, approximately.

B-mode images were captured in long axis view with a frame rate of 25 frames/s and the US beam focalized on the far wall of the carotid artery. The duration of the clips was fixed at 20 s. Mean diameter (Dm) of each vessel was obtained after applying a mathematical contour tracking operator on the images for the automatic location of the edges of the vessel.[20]

Carotid flow was assessed acquiring PW-Doppler data; the velocity measurement range was fixed at 0–5 m/s with the auto tracing option activated while the time scale was fixed at 5 s of analysis in order to acquire five to seven heartbeats. Peak systolic velocity (Vsp), full velocity integral (FVI), and mean velocity (Vm) values were calculated from the envelope of the PW-Doppler trace which was automatically detected by the US equipment.

All parameters were evaluated as means of three measurements. Diameter and velocity values were measured in the right carotid artery at the level of the graft. The evaluations were repeated in the contralateral artery in order to detect possible remodeling effects due to graft implantation. For compliance calculations, the diameter of the carotid artery was measured on a single sheep according to the procedure that was used for the in vitro assays.[20] The systolic and diastolic blood pressure values were obtained by a catheter inserted in the artery of the ear. The compliance of the carotid artery was calculated as the slope of the straight line passing through the two points obtained when plotting pressure versus diameter values.

Color Doppler data were acquired with PRF set to 1.5 kHz and the clip duration fixed at 10 s. These images were used to assess the degree of patency of the graft and to detect hemodynamic abnormalities associated with vascular stenosis[22] in correspondence to the two anastomoses: in particular, the presence of high blood velocities and vortex was subjectively evaluated by an expert operator. Follow-up intervals lasted from the time of surgery until the animals were sacrificed 1, 3, or 6 months later. US evaluation was performed before surgery and, after implantation, on days 7, 14, 21, 30, 60, or 90, and just before the grafts were explanted. No sedation was administered for the US examinations except on the day of the surgery for the first scan before graft implantation.

Animal sacrifice and graft retrieval

At the end of the study, or when grafts were found occluded following US monitoring, animals were sacrificed after heparinization by lethal injection of a barbiturate. As a rule, grafts were explanted with approximately 1–2 cm adjacent segments of carotid artery. Animals that proved to have the grafts patent by US monitoring, were left to go up to the established explant time points of 1, 3, and 6 months (n = 3 for the time points at 1 and 3 months; and n = 4 for the time point at 6 months). The patency of each harvested graft was also assessed by perfusion of physiologic saline solution through the lumen. Then grafts were longitudinally opened on the convex side, passing through both anastomoses, and rinsed carefully with physiologic saline solution. All explanted grafts were macroscopically examined for aneurysm formation, thrombosis, anastomotic failure, and luminal surface appearance. Any local intolerance signs, such as seroma, necrosis, infection, or hemorrhage, were recorded.

An evaluation of the thrombogenicity and the occurrence of fibrous tissue development was conducted. Particular attention was devoted to the presence of intimal hyperplasia (IH) at anastomosis points. Macroscopic photographs were taken of the longitudinally opened grafts to assess the presence and extension of a neointimal lining on the luminal surface.

Finally, specimens were fixed in 10% buffered formalin solution for histological analysis.

Histological analysis

Following 40 h in the fixative, vascular explants were extensively washed under running tap water and transferred to 70% ethanol.

Thereafter, samples were embedded in the light-curing resin Technovit 7200VLC (Kulzer, Bio-Optica, Milano, Italy), infiltrated for 21 days under vacuum, changing the resin every 7 days. Samples were polymerized by the Exakt 520 polymerizator system.

Curing was performed at 450 nm light with the temperature of the specimens never exceeding 40°C. The specimens were then prepared to be cut, according to the precision paralleling-guide procedure protocol, using the precision press Exakt 401 and 402 Vacuum Adhesive Press. Sections were then cut using the Exakt 310 CP cutting unit. The sections obtained were approximately 200 μm in thickness. Sections were then ground to a final thickness of 20–30 μm using the Exakt 400 CS micro grinding unit. Exakt equipment was provided by Exakt Advanced Technologies, Bio-Optica Milano, Italy.

Sections were colored with Hematoxylin/Eosin, Von Kossa, and Stevenel/Van Gieson stains. Hematoxylin/Eosin staining is a sequence of Harris hematoxylin solution (Bio-Optica, Milan, Italy) and 0.25% eosin Y solution (Carlo Erba, Milan, Italy). Von Kossa's staining is a sequence of 1% acqueous silver nitrate (Sigma-Aldrich, St. Louis, MO) solution, 5% sodium thiosulfate (Sigma-Aldrich, St. Louis, MO) and 0.1% nuclear fast red solution for counterstaining. Stevenel/Van Gieson stain is a sequence of Stevenel's blue stain prepared by mixing methylene blue (1%) (Sigma-Aldrich, St. Louis, MO) and potassium permanganate (1.5%) (Carlo Erba, Milan, Italy) dissolved in boiling distilled water. Van Gieson picro-fuschin stain is prepared by first dissolving

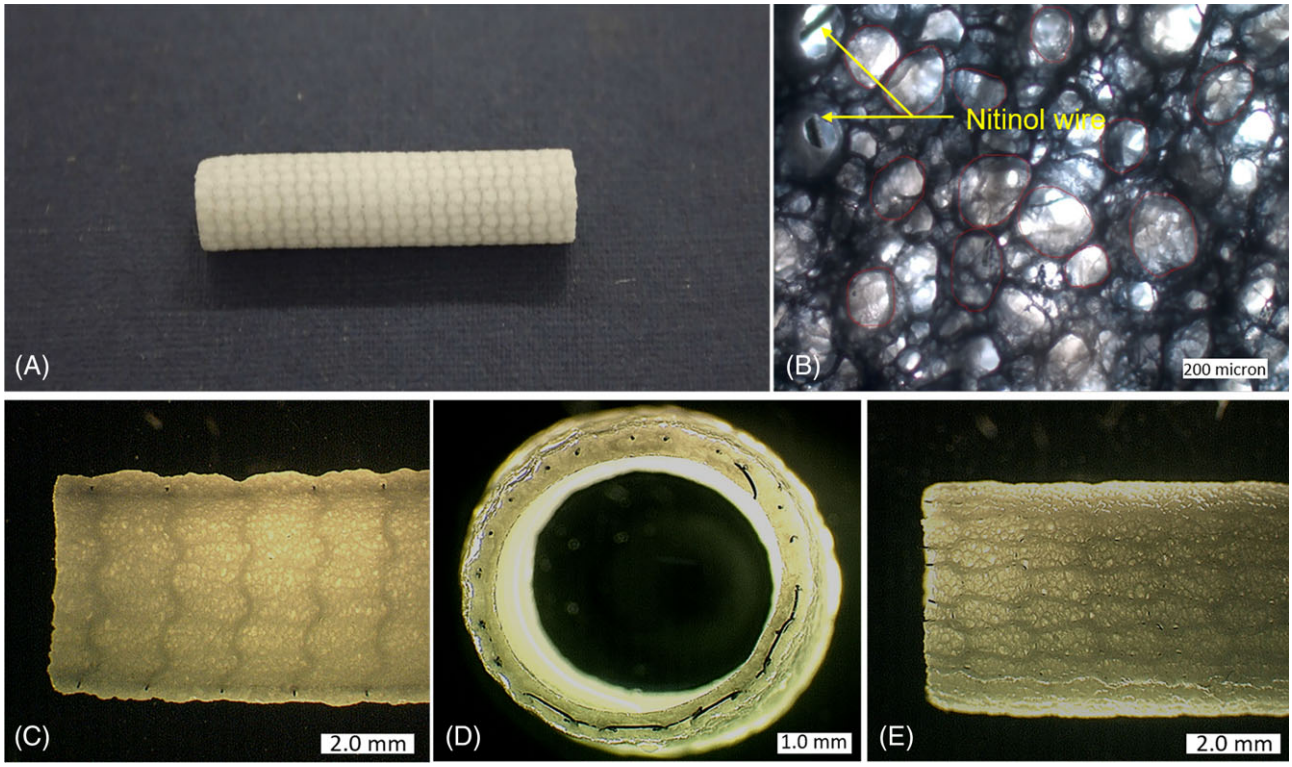

FIGURE 4. Composite view of the Nitinol mesh reinforced graft. A: Macrophotography of a segment of the reinforced graft showing in transparency the embedded Nitinol mesh. B: Stereomicroscope image of a close-up view of a Sudan Black stained outside surface of a reinforce graft showing its highly porous structure (about 140 μm) (red circle). Some Nitinol wires of the mesh are visible through the pores (yellow arrows) (O.M. 50×). C: Stereomicroscope image of the luminal surface of the reinforced graft (O.M. 10×). D: Stereomicroscope image of the cross-section of the reinforced graft (O.M. 15×). E: Stereomicroscope image of the outside surface of the reinforced graft (O.M. 10×).

0.1 g acid fuchsin (Sigma-Aldrich, St. Louis, MO) in 10 ml of distilled water, followed by the addition of 100 mL of saturated picric acid (Nova Chimica Panreac, Milan, Italy). Images were taken using the Axiovert 200 M microscope (Zeiss, Germany) at 200× O.M.

RESULTS

Morphological analysis results

Figure 4(A) shows a microphotographic image of a segment of the vascular prosthesis incorporating the Nitinol mesh. The characteristic woven structure of the Nitinol mesh is visible through the outer surface of the graft wall. Figure 4 (B) shows a stereomicroscope image of the outer surface of a Sudan Black stained graft sample in which, in the blue-dark green range, fibers and a polygonal void of approximately 140 ±43 μm are visible. Nitinol wires can be seen through the voids of the graft wall.

Figure 4(C–E) show low magnification stereomicroscope images of graft sections. Figure 4(C,E) are longitudinal sections of the graft showing, respectively, the luminal surface and the outer surface. Both graft surfaces show a porous structure with evenly distributed pores of comparable pore size. In the longitudinal sections, the characteristic woven structure of the Nitinol mesh is visible through the graft wall on both sides of the graft. Figure 4(D) shows a cross-section of the graft in which catted Nitinol wires of the mesh are visible, extruding from the graft wall section. Catted wires are circularly oriented and positioned approximately in the lower third of the thickness of the graft wall. Due to the highly porous structure of the graft wall, the measured hydraulic permeability was in the order of 40 mL/min/cm^2 at 120 mmHg.

In vitro graft versus in vivo carotid compliance results

Figure 5 shows a plot with cross-sectional area against pressure data, both for the graft (in vitro as circle dots) and for the carotid artery of sheep (in vivo as square dots).

For the in vitro tests, the frequency was fixed to 40 bpm. The diastolic pressure of the VAD was set to 0 mmHg (0 kPa), while the systolic pressure was varied among 6.65, 9.31, 13.3, 15.9, 18.6, and 21.3 kPa in five different tests.

For in vivo tests, the diameter was measured when the pressure was maximal (systole, Ps = 14.8 kPa) and minimal (Pd = 11.8 kPa), respectively.

The linear interpolation (dashed lines) of the in vitro and in vivo data points was 1e-07 + 1e-05 and 8e-08 + 2e-05, respectively. The slope of the interpolation line was considered a surrogate measurement of the compliance that is equal to 1e-07 m^2/kPa for the graft and 8e-08 m^2/kPa for the carotid artery.

In vivo ultrasound imaging results

Examples of B-mode, PW-Doppler and Color Doppler images of the implanted graft obtained from a single sheep are

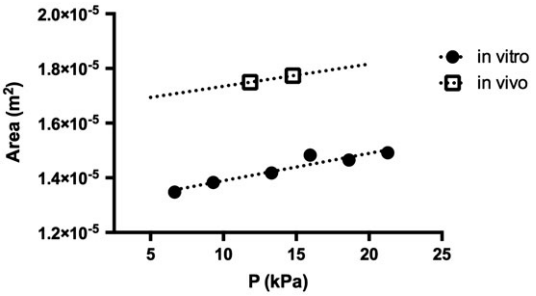

FIGURE 5. Area–pressure plot of both in vitro and in vivo data. Different points refer to different conditions in terms of applied pressure. The area was evaluated form diameter measurement under the hypothesis of circular shape. The slope of the linear interpolation was considered as a surrogate marker of the stiffness of tissue.

shown in Figure 6. US examinations performed at the fixed time points showed that all the grafts were patent. Figure 7 shows mean diameter (Dm) (A), full velocity integral (FVI) (B), peak systolic velocity (Vsp) (C), and mean velocity (Vm) (D) values for each time point. The comparison between the 7 days (first available measurement after surgery) and 30/90/180 days assessments, obtained corresponding to the graft, displayed a progressive reduction in Dm values and a smooth adaptation in the form of an increase of the FVI measurements, despite a flat time course of Vm and Vsp.

At the level of the contralateral carotid artery, the diameter showed a sort of compensatory effect with a small reduction on postsurgical days which slowly recovered during follow-up.

All blood velocity parameters (Vm, Vsp, and FVI) were increased after surgery with respect to the baseline values. On the following observations, Vm and Vsp remained flat, while FVI showed a slight upward trend.

Color Doppler image analysis indicated that 30 days after the surgical procedure one of the animals (11.2%) showed presence of high velocities corresponding to the anastomosis, while presence of vortex was found in five of them (55.6%). Color Doppler results were confirmed (when available, i.e., depending on the time of sacrifice of animals) also at successive time points.

Results of gross observations at implantation and retrieval of grafts

For graft implantation, the standard surgical by-pass technique was used. Grafts were easy to cut and suture despite the Nitinol mesh embedded in their walls. The same surgeon (M.M.) implanted all grafts and the carotid clamp time was 25 ± 1.5 min for all grafts. After clamp release and restoring blood flow through the grafts a pulsatile expansion could be appreciated with the naked eye and also perceptible by palpation. Although the grafts had a highly porous wall, the preclotting carried out before implantation, allowed limited bleeding through the wall, which became uniformly red after perfusion with blood. Bleeding stopped spontaneously after a few minutes without the use of hemostatic agents.

In two out of the 10 animals operated, implanted grafts were found occluded before the time point set for graft retrieval: (1) one animal belonged to the group that was supposed to be explanted at 1 month. In this animal, US monitoring had shown presence of a hematoma at the graft proximal anastomosis, likely due to anastomosis bleeding following the surgical operation. The hematoma was syringed and the graft was patent up to 3 weeks

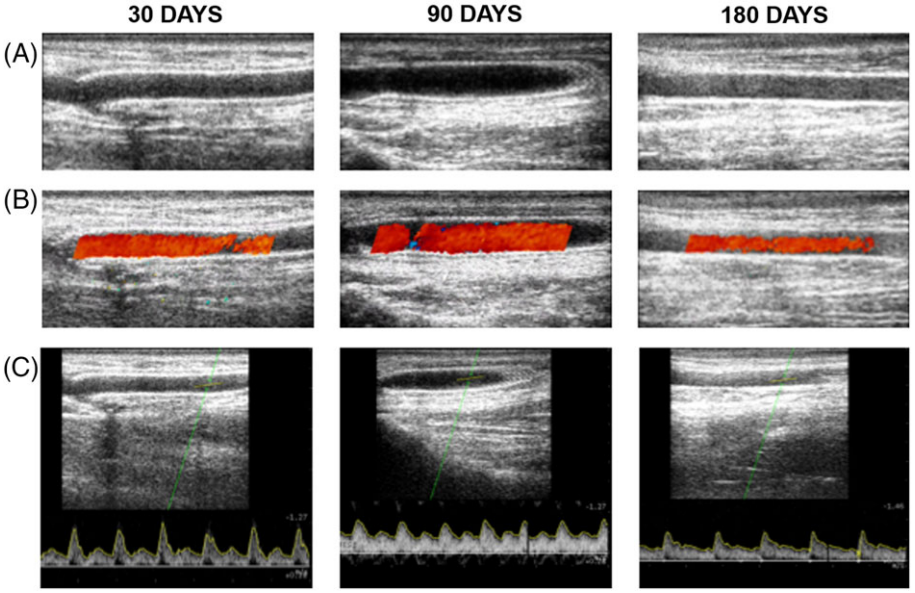

FIGURE 6. Examples of ultrasound images acquired at different time points (columns) and with different ultrasound modalities (B-mode at row A, Color Doppler at row B, and PW-Doppler at row C). Morphological and functional information were available in vivo at 30, 90, and 180 days before the animal's sacrifice. All images were obtained from the same animal with a Mylab 25, Esaote (Italy) equipped with a linear 7.5 MHz ultrasound probe.

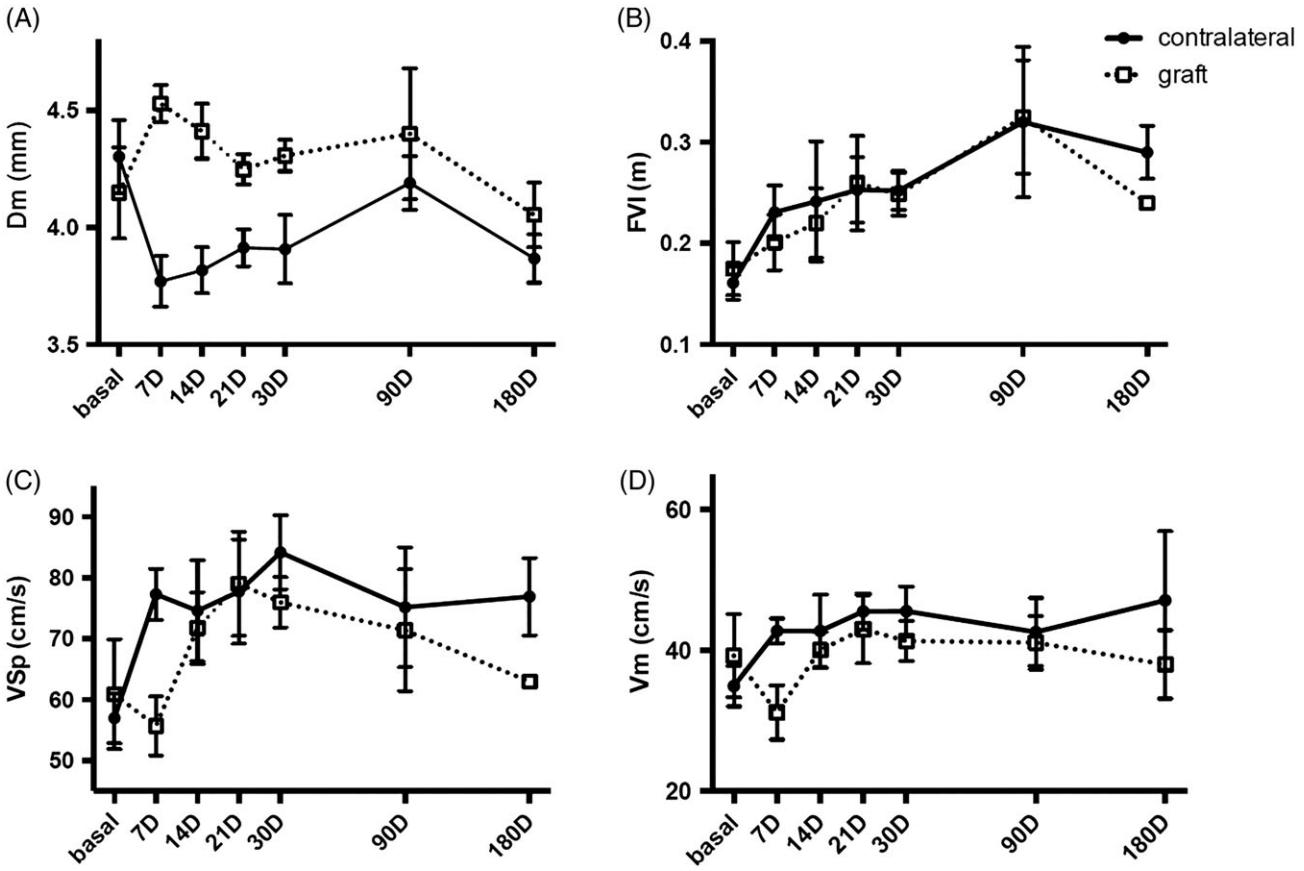

FIGURE 7. Mean diameter (Dm) (A), full velocity integral (FVI) (B), peak systolic velocity (Vsp) (C), and mean velocity (Vm) (D) values for each time point. Measurements related to contralateral vessel and operated vessel in correspondence of the graft insertion are reported. All data are presented as mean and standard deviation. At each time point a different number of animals was considered, according to the experimental design.

postsurgically with good flow. After that it was found occluded and the decision was made to explant it. Gross examination of the longitudinal section of the harvested graft revealed a dark red thrombotic circular formation at the proximal anastomosis filling the area of the "cul-de-sac" and protruding inside the vascular lumen. Two elongated reddish thrombotic formations, attached to the vessel wall and extending from the circular thrombotic mass up to about the middle portion of the vessel, were also visible in the luminal section. From the middle portion up to the distal anastomosis a relatively thrombus-free middle portion was present; with the exception of a relatively white thrombotic formation inside the "cul-de-sac" at the distal anastomosis (figure not shown), (2) the other animal belonged to the group that was supposed to be explanted at 3 months. In this animal, the graft was found occluded at 2 months upon US analysis without any apparent reason. The graft was explanted and gross examination revealed extended red thrombus formation along the graft lumen (figure not shown).

In the remaining eight animals bearing patent grafts, as detected by US monitoring, explants at 1, 3, and 6 months showed a visible expansion of the grafts, indicating good graft functionality. Following ex vivo perfusion no graft offered resistance to flow of saline solution in the lumen. Macroscopic examination of longitudinally opened grafts revealed no aneurysm formation, no massive thrombosis, and no anastomotic failures in any of the grafts explanted at the established time points (Figure 8). No signs of seroma, infection, nor necrosis were observed in any of the animals. The area of the anastomosis did not show macroscopic signs of intimal hyperplasia (IH). Grafts explanted after 1 month showed a relatively thrombus-free luminal surface with graft extremities partially covered by an endoluminal white tissue which extended approximately 2 cm from the proximal anastomosis and 1 cm from the distal one, while the mid-portion appeared largely uncovered with the presence of small portions covered by a thin layer of reddish fibrinous material [-Figure 8(A)]. Grafts explanted after 3 months showed an increase of the extension of the endoluminal white tissue, approximately 3.8 cm from the proximal anastomosis and 2.5 cm from the distal one, both tissues approaching the middle portion of the graft. A small graft middle portion still appeared covered by a reddish fibrinous material at this time point [Figure 8(B)]. All grafts explanted after 6 months a thrombus-free luminal surface covered with a thin endoluminal white tissue reaching confluence in the middle portion of the graft and almost covering its entire luminal surface [Figure 8(C)]. No grafts showed macroscopically

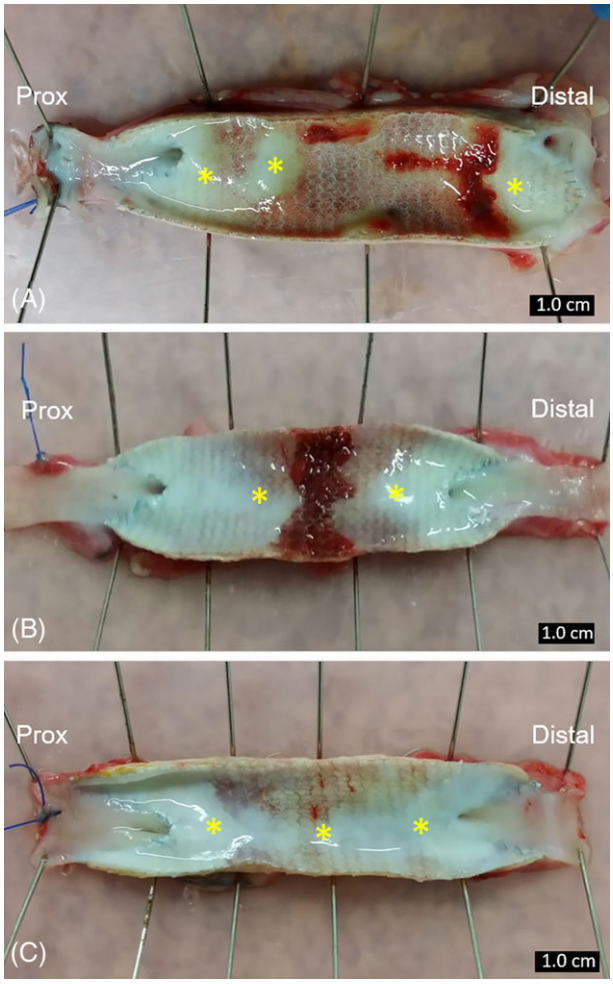

FIGURE 8. Representative macro photographies of the luminal surface of grafts explanted after 1, 3, and 6 months. A: Nitinol reinforced graft after 1 month shows neointima (yellow asterisks) spreading approximately 2.5 cm from the proximal anastomosis and 1.4 cm from the distal one, while the graft middle portion appears largely uncovered. B: Nitinol reinforced graft after 3 months depicts neointima which extends approximately 3.4 cm from the proximal anastomosis and 2.7 cm from the distal one, a reduced graft middle portion appears uncovered. C: Nitinol reinforced graft after 6 months shows the neointima that reaches the confluence in the middle portion of the graft and almost covers the entire luminal surface.

visible signs of calcification. Results of thrombus formation, patency, calcification, and radial enlargement are summarized in Table I.

Histological analysis results

Histological analysis of the grafts explanted after 1, 3, and 6 months showed no significant signs of IH thickening at the carotid-graft anastomoses in any of the explanted samples. At all time points, the outer surface of all grafts appeared widely invaded by fibroblasts from the surrounding tissues (Figures 9–11). Grafts explanted at 1 month and 3 months showed a moderate to intense inflammatory reaction, with macrophages and multinucleated foreign body giant cells (FBGCs) infiltrating the graft wall (Figures 9 and 10). The formation of neo-capillaries in the graft wall was also seen as early as the first month following grafting. Grafts explanted at 6 months showed a significantly reduced inflammatory reaction compared to that visible at 1 and 3 months. The wall of the graft appeared abundantly infiltrated by fibroblasts and interwaved collagen bundles as shown by means of the Van Gieson stain (Figure 12). No detectable inflammatory reaction was seen in the areas around the Nitinol wires. Moreover, no sign of calcification was observed in any of the histological sections by means of the Von Kossa stain (figure not shown).

The luminal side of grafts explanted at 1 month showed neointimal formation at the two anastomoses that originated from the adjacent vessels and grew over the graft luminal surface. The neointima contained fibroblasts and myofibroblast-like cells that integrated with the perivascular tissue infiltrating in the porous graft wall. The middle portion of the grafts showed an unorganized thrombotic layer made of platelets, fibrin and blood cells. No neointimal formation was present in the middle portion at this time point (Figure 9). Observation of grafts explanted at 3 months showed an intimal lining at both anastomoses similar to that observed at 1 month, but with more longitudinally oriented elongated myofibroblast-like cells in respect to the explants at 1 month. In addition, the middle portion of these grafts showed an organized fibrin layer which began to be infiltrated by several myofibroblast-like cells from the transmural cellular tissue ingrowth. The thickness of this immature neointima was 144 $\pm$ 56 μm (Figure 10). Grafts explanted at 6 months showed a similar appearance for all the grafts with an intimal lining along the entire length of the grafts. The neointimal lining appeared abundantly invaded by longitudinally oriented elongated myofibroblast-like cells and also showed an increase in the density of the elongated cells in comparison with that observed in the

TABLE I. Main Macroscopic Findings at Explantation

Implant Time Points	Mesh-Graft 1 mo	Mesh-Graft 3 mo	Mesh-Graft 6 mo
No. sheep	3	3	4
Thrombus formation	0	1[a]	0
Surgical problems	1[b]	0	0
Patency	2	2	4
Calcification	0	0	0
Aneurysmal dilatation	0	0	0

[a]One graft of those planned for the explant at 3 months was found occluded at the 2 months Doppler control without any plausible explanation.

[b]Overall patency 80%. In one graft of those planned for the explant a 1 month it was found presence of hematoma at prox anastomosis, probably due to bleeding. The hematoma was syringed. Graft resulted patent up to 3 weeks with good flow—after that it was found occluded. A dark red thrombotic circular formation was found at proximal anastomosis in the area of "cul-de-sac"—presence of fibrous hard tissue in the area below the "cul-de-sac" near to the proximal anastomosis. A white thrombotic formation inside the "cul-de-sac" was found at distal anastomosis—relatively thrombus free middle portion on the side near to distal anastomosis.

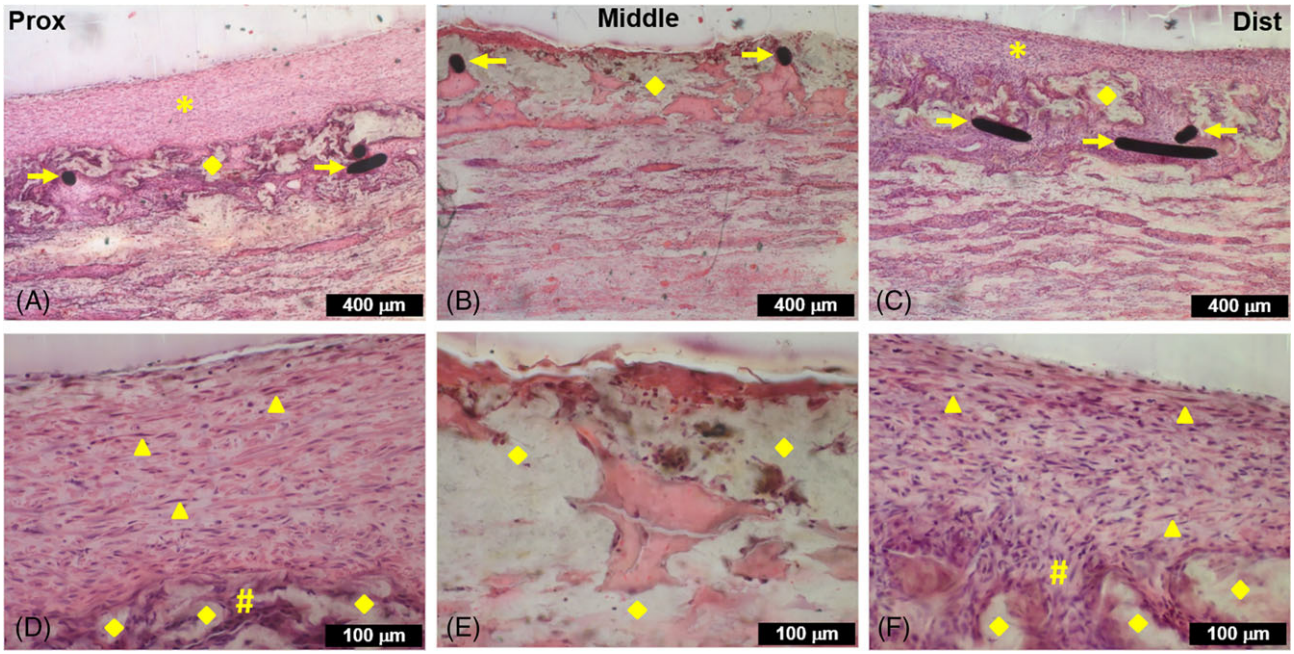

FIGURE 9. Representative histological images of the three portions of the grafts explanted at 1 month. At lower magnification (A–C) (O.M. 50×) a thin neointimal lining is visible both at the proximal (A) and at the distal (C) anastomosis, while the middle portion (B) appears devoid of neointima. At higher magnification (D–F) (O.M. 100×) it is noticeable in both proximal (D) and distal (F) anastomosis, that the neointima contains fibroblasts and myofibroblast-like cells integrated with the perivascular tissue infiltration. The middle portion contains an unorganized thrombotic layer made of platelet, fibrin and blood cells. Legend of the yellow symbols: asterisk = neointima; triangle = myofibroblast-like cells; rhombus = graft material; arrow = Nitinol wire section; hashtag = macrophages. Histological staining: Hematoxylin/Eosin.

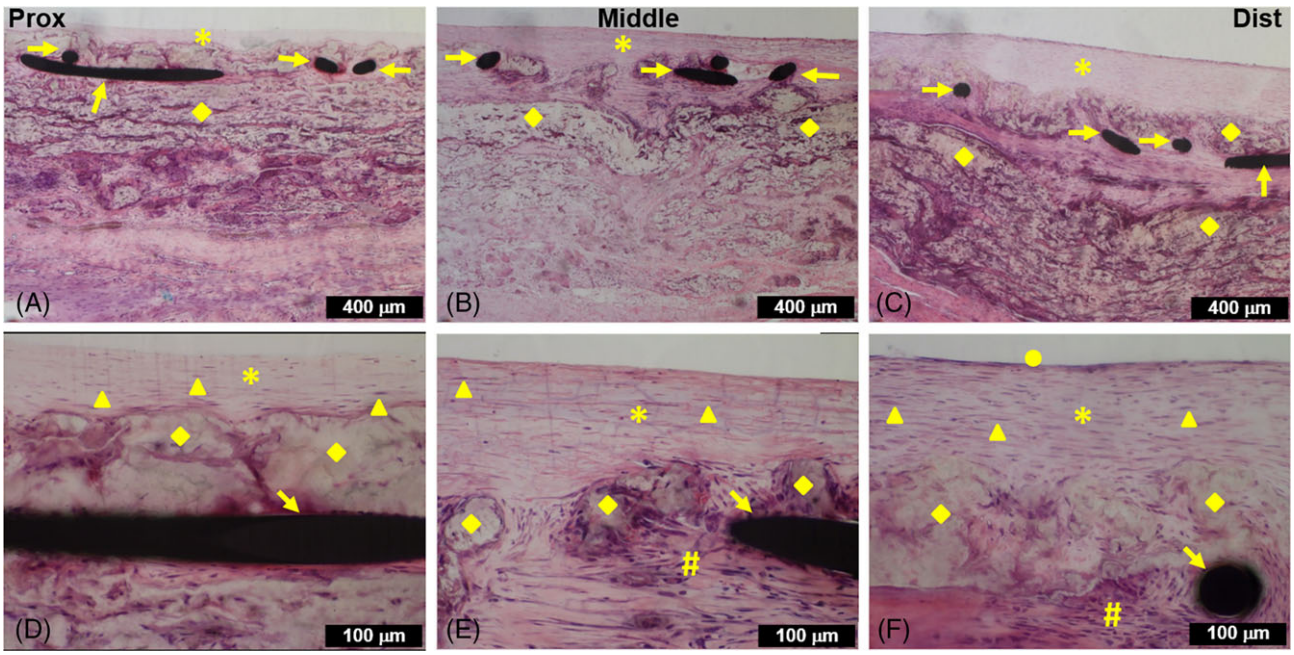

FIGURE 10. Representative histological images of the three portions of the grafts explanted at 3 months. At both lower (A–C) (O.M. 50×) and higher (D–F) (O.M. 100×) magnification grafts show, at proximal [(A) and (D)] and at distal [(C) and (F)] anastomosis, an intimal lining and cellular infiltration qualitatively similar to that observed at 1 month, although more longitudinally oriented elongated myofibroblast-like cell are present at 3 months. Image of the middle portion shows an organized fibrin layer, approximately 144 ± 56 μm thick, containing several myofibroblast-like cells coming from the transmural cellular infiltration. Legend of the yellow symbols: dot = endothelial-like cells; asterisk = neointima; triangle = myofibroblast-like cells; rhombus = graft material; arrow = Nitinol wire section; hashtag = macrophages. Histological staining: Hematoxylin/Eosin.

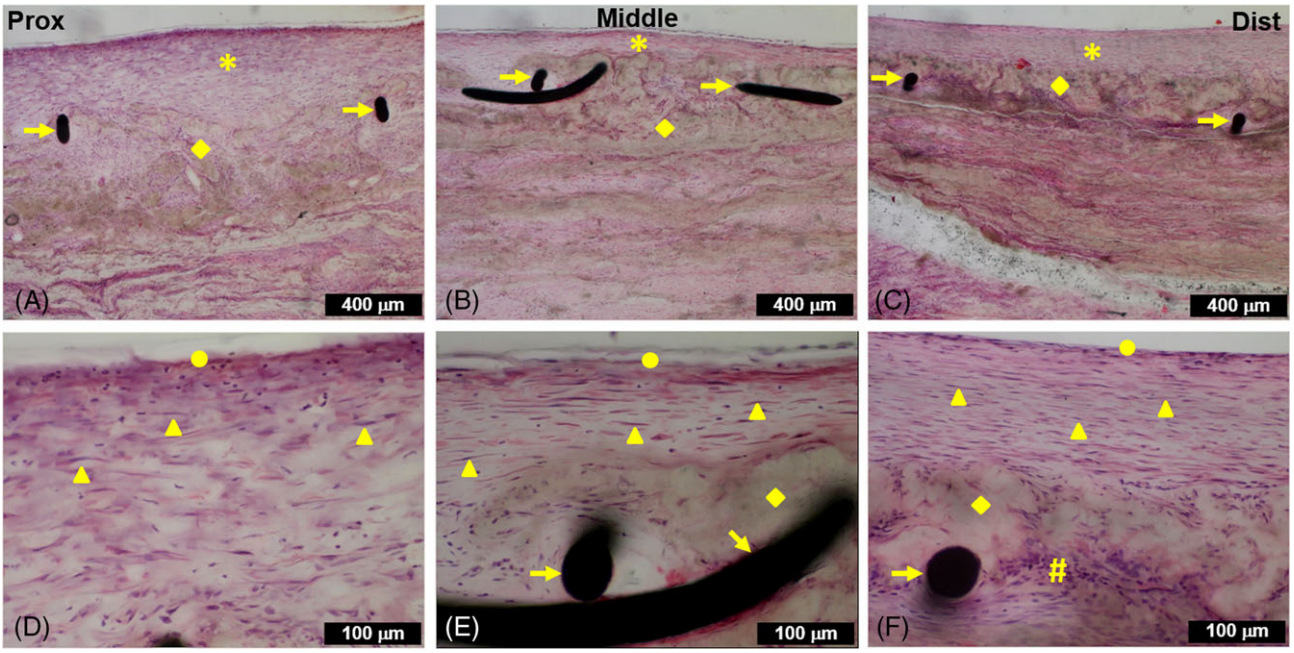

FIGURE 11. Representative histological images of the three portions of the grafts explanted at 6 months. At lower magnification (A–C) (O.M. 50×) all grafts show a similar appearance with an intimal lining along the entire length of the grafts. At higher magnification (D–F) (O.M. 100×) the neointimal lining appears being abundantly invaded by longitudinally oriented elongated myofibroblast-like cell, both at proximal (D) and at distal (F) anastomosis. Elongated myofibroblast-like cell are also abundant in the middle portion where the neointima is rather thinner in comparison with the proximal and distal portion. The thickness of the middle part is approximately 120 ± 46 μm. Endothelial-like cells are visible on-top of the neointimal lining. Legend of the yellow symbols: dot = endothelial-like cells; asterisk = neointima; triangle = myofibroblast-like cells; rhombus = graft material; arrow = Nitinol wire section; hashtag = macrophages. Histological staining: Hematoxylin/Eosin.

explants at 1 and 3 months; this was particularly evident in the middle portion of the grafts where the thickness of the neointima was 120 ± 46 μm. Moderate intimal hyperplasia was observed at the distal anastomosis [Figure 11(C,F)]. Graft neointima lining appeared entirely covered by a layer of endothelial-like cells (Figure 11).

DISCUSSION

In light of our previous experience in the field of vascular prosthesis involving the fabrication and evaluation of PEtU-PDMS SDVG, grafts were produced that were 8 cm in length, 5.0 mm in internal diameter and approximately 500 μm of wall thickness, with two different porous layers in the thickness of the wall: an internal highly porous layer about 100 μm thick, and an external low-porosity layer about 400 μm thick.[12] These grafts were then implanted as bypass grafts in the carotid sheep animal model according to anastomotic techniques used in clinical procedures to bypass the peripheral and coronary arteries. In the contralateral carotid artery, an ePTFE graft of the same internal diameter and length was implanted as control. The study showed better characteristics of the PEtU-PDMS graft in terms of handling, absence of bleeding at the level of stitches, and compliance in comparison with the ePTFE graft. Furthermore, the PEtU-PDMS material showed a capacity of remodeling during the degradation process integrating with the natural tissue by inducing a slight inflammation yet no signs of calcification. PEtU-PDMS grafts explanted after 24 months showed that 80% were patent, with a luminal surface completely covered with a whitish neointima. Although these results appeared encouraging, a disadvantage of these grafts was that in some cases there was a moderate increase in diameter while in others a tendency for aneurysmal dilatation.[12]

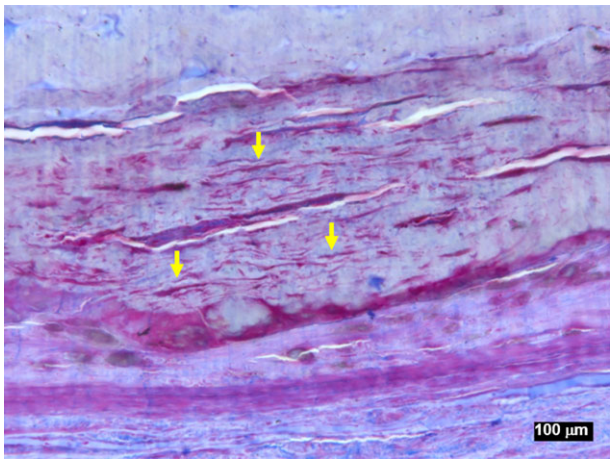

FIGURE 12. Detail of the graft explanted at 6 months showing the presence of collagen bundles (arrows) in the neoformed tissue (O.M. 100×). Histological staining: Stevenel/Van Gieson.

In this study, we tested the feasibility of incorporating a Nitinol mesh into the thickness of the highly porous wall of a synthetic SDVG and we evaluated its degree of patency and endothelialization according to a previously used common carotid artery bypass sheep model. Experimental results showed that incorporating a highly flexible, semicompliant

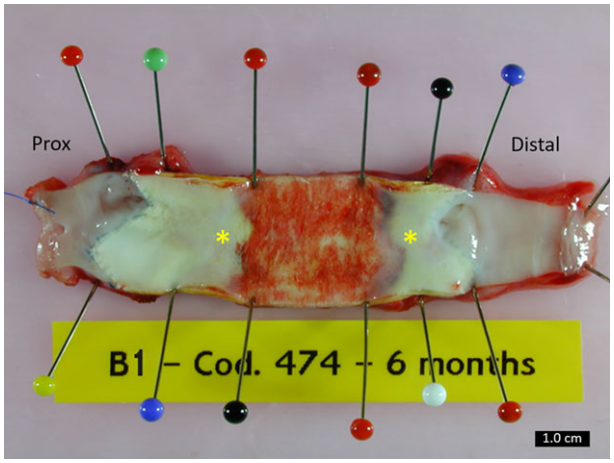

FIGURE 13. Macrophotography of a longitudinally opened PEtU–PDMS impervious, nonreinforced graft after 6 months implantation. This type of graft shows the luminal surface partially covered by a whitish neointima (yellow asterisks) extending approximately 3 cm from the proximal anastomosis and 2 cm from the distal one (Reprinted from Ref. [12], with permission from Elsevier, license number 4092990657490).

Nitinol mesh in the wall of the graft resolved the previously encountered problem of aneurismal dilatation.[12] Grafts reinforced with this technology did not encounter any aneurismal dilatation at the predetermined 1, 3, and 6 months time points. In addition to this, the reinforcement with the Nitinol mesh allowed us to test grafts of smaller size (4.0 mm ID vs. 5.0 mm ID of the previous study) with a highly interconnected porous structure along the graft wall. The reinforced grafts featured an average transmural porosity of about 140 μm and a wall thickness of 350 μm. On the contrary, the nonreinforced grafts used in our previous study featured a total wall thickness of 500 μm composed of a two layer structure: (1) a low porosity (about 30 μm) external fibrolamellar layer 400 μm thick, and (2) a highly porous (about 140 μm) internal microfibrillar layer 100 μm thick.[12] In comparison with the previous study, the 4.0 mm ID, 350 μm thin wall grafts showed a slightly reduced degree of patency (80% vs. 100%); one graft was occluded due to a surgical problem and the other due to an acute thrombus formation. However, the highly porous thinner wall reinforced grafts showed better tissue integration and better degree of endothelialization in comparison with previously used nonreinforced grafts featuring an almost impervious external fibrolamellar layer. This fact is evident from the comparison of the macroscopic observation, at the same explant time point of 6 months, of the luminal surface of the thinner wall, transmurally porous, Nitinol mesh reinforced grafts versus that of the previously used thicker wall, and almost impervious, nonreinforced grafts [see Figure 8(C) vs. Figure 13]. As can be seen from the figures, the graft of Figure 8(C) shows a thin endoluminal white tissue reaching confluence in the middle portion of the graft and almost covering its entire luminal surface, while the graft of Figure 13 shows the luminal surface partially covered by a whitish neointima extending approximately 3.0 cm from the proximal anastomosis and 2.0 cm from the distal one. Furthermore, in Figure 8 (B) the extension of the neointima of a transmural porous Nitinol mesh reinforced graft, explanted after 3 months, is visible. In this graft, only a small central portion of less than 1 cm appears to be devoid of neointima, while the impervious, non-reinforced graft of Figure 13, explanted after 6 months, shows an extension of neointima much lower than the graft of Figure 8(B), considering that graft of Figure 8 (B) was explanted at half the time of that of Figure 13. The results obtained in our study demonstrate a faster neointima formation in the transmurally porous grafts reinforced with the Nitinol meshes, in respect to the impervious non-reinforced grafts.

In our study, particular attention has also been paid to the assessment of compliance by means of noninvasive investigation methods, commonly used in clinical practice. In this context, the compliance of the graft was obtained by US in vitro tests evaluating area changes in correspondence to different changes in pressure. The same methodology was applied to in vivo carotid vessels before surgery, thus allowing a clearer and more complete comparison between the elastic properties of the graft and those of the natural vessel.

In general, the proposed SDVGs compared favorably with other synthetic grafts in terms of compliance. In fact, when the value of compliance was converted to % of compliance per each 100 mmHg, we obtained 4.74%/0.01 mmHg which is higher (then less rigid) in respect to compliance values for expanded polytetrafluoroethylene (0.90%/0.01 mmHg), Dacron (1.90%/0.01 mmHg), and polycaprolactone urethane (1.48%/0.01 mmHg) tubes.[13]

Furthermore, compliance values of human arteries obtained from area and pressure measurements are available in the literature demonstrating the pertinence of the synthetic vessel in representing a valid arterial replacement in terms of elastic features. Accordingly, Castillo-Cruz et al.[13] reported a value of 4.40%/0.01 mmHg for the saphenous vein in humans.

Specifically, the compliance of the graft was found to be very similar to the compliance of the sheep carotid artery (equal to 3.01 when converted in %/0.01 mmHg), which was replaced by the graft itself. As additional confirmation, Shaw et al.[23] reported a compliance value for angiographic normal coronary arteries of 1.3e-7 m^2/kPa, which is very similar to the experimental data obtained with this study.

In view of this last result, we can speculate that the limited presence of restenosis, anastomosis dilatation, and thrombus formation can be ascribed to the good match between the mechanical characteristics of the implanted graft in respect to the natural vessel.

Looking at the morphological US in vivo results, the diameter of the graft measured postsurgery was similar to the replaced natural vessel diameter. During follow-up diameter monitoring, a progressive narrowing can be observed. The narrowing of the lumen reflects the growth of a neointimal lining inside the graft; furthermore, the thickness at the end of the experiment, is compatible with the thickness of the neointimal lining as evaluated by histology. The unoperated vessel seems to inversely adapt its diameter to the change in diameter of the graft, first showing a postsurgery

reduction to compensate the absolute increase in diameter in the operated section, followed by a progressive dilation associated with the internal lining of the graft.

Vm and Vsp values were virtually identical at baseline, but they were found to be different after 7 days postsurgery, in contrast, the contralateral vessel showed higher values in respect to the graft. These results are not surprising due to the larger diameter of the graft. The difference between Vm (Vsp) as measured inside the graft and inside the contralateral vessel was reduced but was still present until the end of the experiment, mirroring the progressive realignment of the diameter of the two vascular sites.

On the contrary, FVI values which represent a global contribution of the blood flow velocity to total blood flow, showed no abrupt changes postsurgery but a steady growth. The absence of abrupt variation in FVI which is noted in Vm and Vsp values after surgery, could be associated with the physical meaning of the FVI parameter that represents the overall blood content delivered from vessels during the whole cardiac cycle, regardless of the shape of the time course of the blood flow velocity. The growth of the FVI both in the operated and in the contralateral vessels, apparently lead to a new stationary point (at 180 days after surgery) characterized by a higher value of the FVI compared to the basal ones in both vascular sides of the sheep. This fact can be explained by the simultaneously stationary working conditions reached by the diameter of the vessels which were different with respect to the pre-operative state, where both graft and contralateral vessels reduced in diameter. Therefore, we could speculate that, at 6 months after surgery, the two branches of the afferent cerebral circulation found a new stable hemodynamic equilibrium characterized by a global reduced diameter with a consequent increase of FVI. This condition would be compatible with a global blood supply to the brain that is comparable before and after surgery.

LIMITATIONS

Our study followed the guidelines of the 3R principle" (reduce, refine, replace) for more ethical use in animal testing[24] and because of that there may have been the limitation of a relatively small number of animals per each time point and, consequently, a limited statistical significance. However, the total number of sheep we used was 10 and this allowed us to test, to the best of our knowledge, for the first time the feasibility of a Nitinol mesh incorporation into a highly porous wall of a synthetic SDVG (4.0 mm ID) and to evaluate its performance in the common carotid artery sheep model.

CONCLUSIONS

The results of this study reinforce previous observations about the key role played by transmural porosity in affecting the performance of SDVGs, demonstrating a higher extension of the neointima luminal coverage in transmurally porous grafts reinforced with the Nitinol meshes, with respect to impervious non-reinforced grafts at the same time point.

In addition, this study demonstrated that ultrasound techniques can be used to quantify and monitor highly informative morphological (diameter) and functional (compliance and blood flow velocity) graft parameters in an experimental model in which the natural vessel is replaced with a synthetic one. This overcomes the typical use of the ultrasound Doppler which is limited to test the vessel patency.[25–27] Furthermore, the noninvasive nature of the ultrasound will allow planning future studies in which the animals' sacrifice is replaced by a multiple time point analysis, in order to reduce the total number of animals required to reach satisfactory statistical power for the study.

Although other factors may affect the degree of endothelialization of a vascular graft, we demonstrated that transmural porosity can play an important role in modulating the speed through which this process takes place in a PEtU-PDMS SDVG. However, to achieve the ambitious goal of having a fast rate of endothelialization in relatively long grafts, such as those needed for the aorto-coronary bypass, further studies will be required aimed at optimizing transmural graft porosity, mesh material properties and likely mesh geometrical design. This can be largely achieved through new mesh materials selection and mesh structural analysis performed with the aid of modern computer information technology, such as CAD, FEM simulation and compliance/mechanical bench-testing. In the end, it is also worth mentioning that besides the very useful in silico and bench-test studies, it will still be necessary to validate the results by implanting the graft in a suitable animal model.

ACKNOWLEDGMENTS

We thank Mr. Eric Solien, Director of Research & Development at Kips Bay Medical, Inc., 3405 Annapolis Lane, Minneapolis, MN 55447, USA, for graciously supplying the Nitinol meshes. Furthermore, we thank Dr. Silvia Burchielli, Veterinary Doctor at "Fondazione Toscana Gabriele Monasterio", Via Trieste 41, 56126 Pisa, Italy, for her precious support during all animal experimentation. The authors also thank Dr. Karin Tyack for her assistance in editing of English language.

DISCLOSURES

Authors did not have any personal or professional relationship with the sponsoring company Kips Bay Medical, Inc. However, the Institute of Clinical Physiology received a Research Grant from the sponsor to perform the animal study.

Abbreviations

CABG	coronary artery bypass graft
CAD	computer aided design
eSVS	external saphenous vein support
FEM	finite element method
ID	internal diameter
PDMS	polydimethylsiloxane
PetU	poly(ether-urethane)
SDVG	small-diameter vascular grafts

REFERENCES

1. Gotto AM, Farmer JA. Risk factors for coronary artery disease. In: Braunwald E, editor. Heart Disease, A Textbook of Cardiovascular Disease. Philadelphia, PA: WB Saunders Company; 2010. pp. 1153–1195.
2. Davies SW. Clinical presentation and diagnosis of coronary artery disease: stable angina. Br Med Bull 2001;59:17–27.
3. Piccolo R, Giustino G, Mehran R, Windecker S. Stable coronary artery disease: Revascularisation and invasive strategies. Lancet 2015;386:702–713.
4. McNeely C, Markwell S, Vassileva C. Trends in patient characteristics and outcomes of coronary artery bypass grafting in the 2000 to 2012 Medicare Population. Ann Thorac Surg 2016;102:132–138.
5. Zhang Z, Wang Z, Liu S, Kodama M. Pore size, tissue ingrowth, and endothelialization of small-diameter microporous polyurethane vascular prostheses. Biomaterials 2004;25:177–187.
6. Eberhart A, Zhang Z, Guidoin R, Laroche G, Guay L, De La Faye D, Batt M, King MW. A new generation of polyurethane vascular prostheses: Rara avis or ignis fatuus? J Biomed Mater Res 1999;48: 546–558.
7. Xu W, Zhou F, Ouyang C, Ye W, Yao M, Xu B. Mechanical properties of small-diameter polyurethane vascular grafts reinforced by weft-knitted tubular fabric. J Biomed Mater Res A 2010;92:1–8.
8. Yang H, Zhu G, Zhang Z, Wang Z, Fang J, Xu W. Influence of weft-knitted tubular fabric on radial mechanical property of coaxial three-layer small-diameter vascular graft. J Biomed Mater Res B Appl Biomater 2012;100:342–349.
9. Xie X, Eberhart A, Guidoin R, Marois Y, Douville Y, Zhang Z. Five types of polyurethane vascular grafts in dogs: the importance of structural design and material selection. J Biomater Sci Polym Ed 2010;21:1239–1264.
10. Emery RW, Solien E, Jamieson SW. Implantation of the eSVS mesh. Innovations (Phila) 2012;7:65–67.
11. The eSVS® Mesh Randomized Post-Market Study. ClinicalTrials.gov Identifier: NCT01462721.
12. Soldani G, Losi P, Bernabei M, Burchielli S, Chiappino D, Kull S, Briganti E, Spiller D. Long term performance of small-diameter vascular grafts made of a poly(ether)urethane–polydimethylsiloxane semi-interpenetrating polymeric network. Biomaterials 2010;31: 2592–2605.
13. Castillo-Cruz O, Pérez-Aranda C, Gamboa F, Cauich-Rodríguez JV, Mantovani D, Avilés F. Prediction of circumferential compliance and burst strength of polymeric vascular grafts. J Mech Behav Biomed Mater 2018;79:332–340.
14. Khodadoust M, Mohebbi-Kalhori D, Jirofti N. Fabrication and characterization of electrospun bi-hybrid PU/PET scaffolds for small-diameter vascular grafts applications. Cardiovasc Eng Technol 2018;9:73–83.
15. Briganti E, Losi P, Raffi A, Scoccianti M, Munaò A, Soldani G. Silicone based polyurethane materials: a promising biocompatible elastomeric formulation for cardiovascular applications. J Mater Sci Mater Med 2006;17:259–266.
16. Soldani G. Elastomeric material and process for preparation thereof. U.S. Patent 7,157, 118 B2, 2nd January, 2007.
17. Soldani G, Panol G, Sasken HF, Goddard MB, Galletti PM. Small diameter polyurethane–polydimethylsiloxane vascular prostheses made by a spraying, phase-inversion process. J Mater Sci Mater Med 1992;3:106–113.
18. Okoshi T, Chen H, Soldani G, Galletti PM, Goddard M. Microporous small diameter PVDF–TrFE vascular grafts fabricated by a spray phase inversion technique. ASAIO J 1992;38:M201–M206.
19. Soldani G, Losi P, Milioni C, Raffi A. Light microscopy evaluation of polyurethane vascular grafts porosity by Sudan black b staining: An alternative to standard scanning electron microscopy. J Microsc 2002;206:139–145.
20. Gemignani V, Faita F, Ghiadoni L, Poggianti E, Demi M. A system for real-time measurement of the brachial artery diameter in B-mode ultrasound images. IEEE Trans Med Imaging 2007;26: 393–404.
21. Wesly RL, Vaishnav RN, Fuchs JC, Patel DJ, Greenfield JC Jr. Static linear and nonlinear elastic properties of normal and arterialized venous tissue in dog and man. Circ Res 1975;37:509–520.
22. Hua Y, Meng XF, Jia LY, Ling C, Miao ZR, Ling F, Liu JB. Color Doppler imaging evaluation of proximal vertebral artery stenosis. AJR Am J Roentgenol 2009;193:1434–1438.
23. Shaw JA, Kingwell BA, Walton AS, Cameron JD, Pillay P, Gatzka CD, Dart AM. Determinants of coronary artery compliance in subjects with and without angiographic coronary artery disease. J Am Coll Cardiol 2002;39:1637–1643.
24. Russell WMS, Burch RL. The Principles of Humane Experimental Technique. London, UK: Methuen; 1959. ISBN:0900767782.
25. Ma X, He Z, Li L, Liu G, Li Q, Yang D, Zhang Y, Li N. Development and in vivo validation of tissue-engineered, small-diameter vascular grafts from decellularized aortae of fetal pigs and canine vascular endothelial cells. J Cardiothorac Surg 2017;25:101.
26. Jaramillo J, Valencia-Rivero KT, Cedano-Serrano FJ, López R, Sandoval N, Briceño JC. Design and evaluation of a structural reinforced small intestinal submucosa vascular graft for hemodialysis access in a porcine model. ASAIO J 2018;64:270–277.
27. Hu YT, Pan XD, Zheng J, Ma WG, Sun LZ. In vitro and in vivo evaluation of a small-caliber coaxial electrospun vascular graft loaded with heparin and VEGF. Int J Surg 2017;44:244–249.